Observing the Effects of Temperature and Surface Roughness on Cetyltrimethylammonium Bromide Adsorption Using Quartz-Crystal Microbalance with Dissipation Monitoring

Joshua J. Hamon[†], Alberto Striolo[‡], and Brian P. Grady[†*]

[†]*School of Chemical, Biological and Materials Engineering and Institute of Applied Surfactant Research, University of Oklahoma, 100 East Boyd St., Norman, Oklahoma 73019.* [‡]*Department of Chemical Engineering, University College London, London WC1E 7JE*
**corresponding author.*

Phone: 001-405-325-4369; Fax 001-405-325-5813
Email: jjhamon16@gmail.com, a.striolo@ucl.ac.uk, bpgrady@ou.edu

Corresponding author. Tel: 405-325-4369; fax: 405-325-5813; Email: bpgrady@ou.edu

Acknowledgements

The authors acknowledge financial support from the industrial sponsors of the Institute for Applied Surfactant Research (IASR) at the University of Oklahoma. The sponsoring companies for the Institute of Applied Surfactant Research are Church & Dwight, Clorox, Colgate-Palmolive Company, Ecolab, Flotek Chemistry, Huntsman Corporation, Procter & Gamble, Sasol (USA) Corporation and Shell Global Solutions (US) Inc.. The National Science Foundation also supported this research under Grant No. CMMI–1068705. The authors would also like to thank Dr. Mark Poggi and Dr. Elizabeth Scheider of Q-sense for help in obtaining rough crystals and Dr. Matthew Dixon for guidance pertaining to the QCM and data analysis.

Abstract

The effects of temperature and surface roughness on the mass and viscoelasticity of an adsorbed surfactant layer were monitored using the quartz crystal microbalance with dissipation monitoring (QCM-D). Adsorption isotherms at 30, 40, 50 and 60°C and at two different roughnesses on gold were measured for cetyltrimethylammonium bromide (CTAB). All isotherms displayed an increase in mass and dissipation as surfactant concentration was increased to its critical micelle concentration (CMC). Above the CMC adsorption reached a peak followed by a slight decrease to a plateau at the equilibrium adsorption value. As the temperature was increased the adsorbed mass above the CMC decreased. The adsorbed mass decreased further by increasing substrate roughness, while the dissipation remained unchanged within experimental uncertainty.

Dynamic adsorption experiments were also conducted at various temperatures for select concentrations above and below the CMC, providing evidence of the importance of different adsorption mechanisms as a function of both surfactant concentration and surface roughness.

Keywords: Adsorption Isotherm, Cationic Surfactants, Surface Activity, Adsorption Kinetics

1. Introduction

Surfactants are economically useful in applications such as mineral flotation, regeneration of carbon found in adsorption beds, detergency, oil recovery and de-inking of paper in recycling.(Paria and Khilar, 2004) Adsorption at the solid-liquid interface is controlled by several factors including the electrostatic nature of the surfactant head group, hydrophobic chain length, branching of the hydrophobic chain, temperature, characteristics of the solid (i.e. roughness, surface charge etc.) and the characteristics of the solvent (polarity, chemical additives, pH, etc.).(Dixit, et al., 2002; Salari, et al., 2011; Wu, et al., 2011) Among the main interactions that lead to surfactant adsorption are electrostatic interactions between the surfactant head group and the substrate surface, and hydrophobic interactions between the substrate and adjacent surfactant molecules.(Alkan, et al., 2005; Marsalek, et al., 2011)

The quartz crystal microbalance with dissipation monitoring (QCM-D) has proven to be a useful tool for probing concentration and time-dependent mechanics of surfactant adsorption on a surface under a variety of conditions. Traditionally, surfactant adsorption has been quantified using ellipsometry, surface plasmon resonance, neutron reflectivity and a variety of gravimetric techniques involving textile fabrics, clay and other minerals.(Caruso, et al., 1995; Fragneto, et al., 1996; Gürses, et al., 2010; Marsalek, Pospisil and Taraba, 2011; Seidel, et al., 1996; Stålgren, et al., 2002)

Several publications reported the difference between QCM-D and optical methods for measuring the amount of surfactant adsorbed from bulk solutions.(Bordes, et al., 2010; Howard and Craig, 2009; Macakova, et al., 2007; Mivehi, et al., 2011) Although QCM has been found to report higher adsorbed masses than optical methods, there is some debate as to whether solvent entrapped in the adsorbed layer is the cause. Macakova et al. hypothesized that entrapped solvent, specifically “hydration” solvent surrounding the surfactant head groups, was negligible

when the cationic surfactants CTAB and two closely related analogues were used, but solvent trapped in the cavities caused by surface roughness (mechanically trapped) must be considered. The presence of trapped water had no effect on the dissipation of adsorbed layers unless the organization of the surfactant layer on the surface of the substrate changes.(Macakova, Blomberg and Claesson, 2007)

Our group postulated that the over-estimation of the adsorbed mass sensed by QCM-D is not caused solely by trapped solvent, but also by a difference between the roughness of the surfaces used by QCM and other techniques.(Gutig, et al., 2008) Our hypothesis stems from the fact that the typical substrates used in optical methods are extremely smooth when compared to those used in QCM experiments, as assessed by root-mean square roughness measurements, and therefore by using the nominal (non-roughness corrected) surface area there would appear to be a greater amount adsorbed per unit area, leading to the misconception of entrapped solvent.(Stålgren, Eriksson and Boschkova, 2002) Following our interpretation, when the roughness corrected surface area was used, the mass adsorbed per unit area actually decreased vs. a smooth surface.(Macakova, Blomberg and Claesson, 2007; Sakai, et al., 2010; Wu, et al., 2011)

Surface roughness could cause other phenomena. For example, Fragneto et al. found that CTAB formed a bi-layer on both smooth and rough silicon surfaces, but that the surfactant film on the rough surface displayed an increase in the bi-layer thickness and a decrease in surface coverage and degree of packing between adjacent surfactant molecules when compared to the smooth surface.(Fragneto, et al., 1996) These and other surface roughness effects are attributed to disruption of the hydrophobic interactions between surfactant tails, which is the primary driving force for adsorption near the critical micelle concentration (CMC), as well as a decrease

in the number of surface sites favorable to adsorption.(Fragneto, et al., 1996; Gutig, Grady and Striolo, 2008; Somasundaran and Huang, 2000; Wu, et al., 2011)

Under ambient conditions, gold surfaces are made hydrophobic by the physisorption of organics.(Smith, 1980) However, the gold substrates used in our experiments have been found to have a surface that is primarily hydrophilic, which has been shown to induce CTAB adsorption in the form of cylindrical aggregates.(Jaschke, et al., 1997; Saphanuchart, et al., 2007; Wall and Zukoski, 1999) Other studies have shown that gold and various other hydrophobic surfaces have supported the formation of bi-layer films characteristic of a hydrophilic surface, although in some cases this was done purposefully by the addition of co-solutes.(Fragneto, et al., 1996; Gutig, Grady and Striolo, 2008; Shi, et al., 2009) The hydrophilic nature of the surface used in our experiments was found to be caused by the high concentration of oxygenated sites and the adsorption of halide ions, which have been reported previously by ours and other groups to create a negative charge on the surface.(Knag, et al., 2005; Mivehi, Bordes and Holmberg, 2011; Wu, et al., 2011) The gold surface provided by the manufacturer displays hydrophilic character even on the uncleaned surface, although further oxygenation and hydrophilicity is caused by the recommended cleaning procedure (RCA-1 solution), which has been shown to increase the hydrophilicity of silicon as well.(Bordes, Tropsch and Holmberg, 2010; Cademartiri and Ozin, 2009; Gutig, Grady and Striolo, 2008; Hermansson, et al., 1991)

The effect of temperature on surfactant adsorption has been studied in the literature. These studies show, for example, that for ionic surfactants the adsorption process is exothermic.(Gürses, et al., 2010; Partyka, et al., 1993; Seidel, Wittrock and Kohler, 1996; Somasundaran and Krishnakumar, 1997) Several published works discuss the inverse temperature dependence of ionic surfactants, i.e. as the temperature is increased the maximum equilibrium adsorption for ionic surfactants decreases.(Alkan, et al., 2005; Biswas and Chattoraj,

1998; Fava and Eyring, 1956; Gürses, et al., 2010; Meader and Fries, 1952; Myers, 2006; Paria and Khilar, 2004; Pavan, et al., 1999; Rosen, 2004; Seidel, Wittrock and Kohler, 1996) This behavior is caused by a decrease in the positive entropy change upon adsorption, caused by a reduction in order of the cage-like structure of water molecules around the surfactant tails at higher temperatures.(Gürses, et al., 2010; Paria and Khilar, 2004; Pavan, et al., 1999; Ruiz and Molina-Bolivar, 2010)

In terms of experiments at different temperatures, Krafft temperature and CMC changes are both important to consider. The Krafft temperature is the temperature at which surfactant solubility matches the CMC. (Manojlovic, 2012) The Krafft temperature of aqueous CTAB lies between 20°C and 25°C, and varies because of the presence of other compounds or contaminants in solution.(Beyer, et al., 2006; Manojlovic, 2012; Vautier-Giongo and Bales, 2003)

In this work the effects of changing temperature and surface roughness on surfactant adsorption were studied simultaneously using the QCM-D and the cationic surfactant CTAB on a gold surface. Observations were made using isotherms at 4 different temperatures and two different surface roughnesses. In addition, time-dependent data were collected and the average slopes in different regions of adsorption were calculated using a simple model.

2. Experimental Procedures

2.0 Materials

Cetyltrimethylammonium bromide was purchased from Sigma Aldrich at approximately 99% purity. CTAB was purified by re-crystallization three times in HPLC grade ethanol to remove impurities before using it to prepare a 15 mM stock solution with Milli-Q H_2O (18 MΩ cm), purified using an arrangement of Milli-Q ion-exchange and activated carbon filters.

Surfactant solutions were diluted in glass vials, which were previously cleaned in sulfuric acid containing Nochromix©. The CMC of CTAB was measured at various temperatures using a Mettler Toledo Seven Multi conductivity meter and plotting specific conductivity vs. concentration to find the break point in the slope.(Dominguez, et al., 1997; Manna and Panda, 2011; Mata, et al., 2005)

Quartz crystals were purchased from Q-Sense. The smooth crystals (QSX 301) are layered with ~100 nm of gold and have a nominal frequency of 5 MHz. The rough crystals (QSX 999 Au Rough) were prepared specially for our group by Q-Sense and also have a nominal frequency of 5 MHz.

2.1 Roughness Characterization

Roughness measurements on the crystal surfaces were performed with the Agilent 5420 Atomic Force Microscope. Images were obtained in air using the NSC15/ALBS silicon nitride cantilevers from MicroMasch, with force constant 46 N/m and resonant frequency 325 kHz and tip size less than 8 nm. Scan sizes were 2 μm × 2 μm and the pixel resolution was 512 × 512 pixels, taken at scan frequencies < 1 Hz. Root-mean square (RMS) roughness values are reported as the average for 3 independent areas on either a single smooth or rough crystal. An example of an AFM image of a smooth crystal is shown Figure 1. The reported RMS data are averaged over two similar crystals and the error reported for each crystal below was found as the standard deviation. Before undergoing any washing procedures, the RMS roughness of the smooth crystals was found to be 0.9 ±0.07 nm, which agrees well with the manufacturer's reported value of 0.9 ± 0.2 nm. Following the cleaning procedure, the roughness of the smooth crystal had increased to 2.13 ±0.19 nm. The rough crystals (QSX 999 Au) had an RMS value of 5.72 ± 0.16 nm before the cleaning protocol; following a cleaning procedure the roughness increased to 6.17 ± 0.23 nm. The roughness increase following cleaning is likely due to the RCA

solution attacking high energy sites on the surface of the crystal more than the low energy sites causing the creation of additional "peaks and valleys" and creating a rougher surface with each washing.

All data presented in this paper were obtained assuming the nominal, not the actual surface areas of the sensing elements. Previously an RMS of 5.8 nm was considered to represent a surface area of 10.12 μm^2 (compared to a nominal 4 μm^2), using a fractal approach to calculate the surface area based on roughness measurements.(Wu, et al., 2011)

2.2 Cleaning Procedures

Washing protocols are divided into smooth and rough crystal sections for clarity, although both procedures follow similar steps.

2.2.1 Smooth Crystals: Crystals were used a maximum of four times because adsorption did not change significantly during the four runs; in a few cases crystals gave results very different than the results from the previous trial; in this case the crystal was discarded even if four runs had not been completed. The crystals were placed in a Harrick Plasma Cleaner (PDC-32G) and cleaned using the medium setting (10.5 W applied to RF coil) in air for 10 minutes. The crystals were then transferred to a Q-Sense sensor Teflon© holder and immersed in an 80 °C RCA-1 cleaning solution (1:1:5 solution of NH_4OH:H_2O_2: Milli-Q H_2O) for 5 minutes.(Cademartiri and Ozin, 2009; Hermansson, et al., 1991) The sensors were removed from the solution and rinsed individually with Milli-Q H_2O and dried under a nitrogen stream. The crystals were then immediately moved to the plasma cleaner for 5 minutes on the low setting (6.8 W applied to RF coil). Finally, the sensors were moved from the plasma cleaner directly into a QCM module for immediate measurement.

2.2.2 Rough Crystals: Rough crystals were removed from the box and placed directly into an RCA-1 cleaning solution at 80 °C for 5 minutes. Afterwards the crystals were removed and

individually rinsed and dried using the same procedure employed on the smooth crystals. They were then placed into a fresh RCA-1 solution at 80 °C for another 5 minutes, then rinsed and dried. This procedure was repeated once more before placing the crystals in their modules as in the smooth crystal procedure. Rough crystals were only used once because the adsorption changed with subsequent cleanings. No plasma cleaning was performed on the rough crystals as it was found to alter the crystal surface area in our previous experiments.(Wu, et al., 2011)

2.3 QCM-D Data Collection and Experimental Protocol

The interpretation of QCM data is provided extensively in the literature.(Bordes and Hook, 2010; Bordes, Tropsch and Holmberg, 2010; Howard and Craig, 2009; Kou, et al., 2010; Stålgren, Eriksson and Boschkova, 2002) During our measurements we observed that the data gathered from the first and third overtones for the oscillation frequency were routinely erratic and therefore were discarded; the 5^{th} - 13^{th} overtones were used to determine mass and dissipation values. Changes in mass adsorbed and dissipation were measured for CTAB at, 30 °C, 40 °C, 50 °C, and 60 °C using the Q-sense E4 microbalance. The temperature was controlled within ±0.05 °C of the desired setpoint.

A peristaltic pump using Tygon© tubing was used to draw surfactant solutions through Teflon© tubing into the modules at a rate of 0.1 mL/min. At the beginning of each experiment cleaned sensors were placed in their modules and pure Milli-Q water was used to obtain stable baseline frequency and dissipation values, (noted by a change in frequency of less than 0.03 Hz/min). The pump flow direction was toggled periodically during equilibration to dislodge bubbles that sometimes formed on the crystal and tubing surfaces.

Once a stable baseline was acquired, the pump was stopped long enough to remove the tubing from the pure water and immediately placed in the vial containing a CTAB solution. Just prior to injection, each new concentration increment was sonicated for 10 minutes and then

heated to within 5° C of the desired temperature, while being sparged with helium to remove as much dissolved gas as possible.

In one set of measurements, adsorption isotherms were measured. During each isotherm the surfactant concentration was increased in increments of 0.1 CMC of CTAB until 0.6 CMC was reached. From there the concentration was increased by 0.2 CMC up to a bulk concentration of 2.0 CMC and then increased in one step to a bulk concentration of 2.5 CMC. All QCM measurements are susceptible to drift over time, which can introduce error and make the determination of equilibrium difficult. Equilibrium was considered achieved when the change in frequency for all crystals fell within 0.03 Hz/min. The time needed to reach equilibrium ranged from 15-20 minutes for the higher concentrations to 30-45 minutes for the lowest concentrations. After equilibrium was reached, a new concentration was drawn through the apparatus by stopping the pump and moving the tubing to a new vessel containing the desired concentration.

In separate kinetic experiments, mass adsorbed on gold as a function of time was recorded. In these experiments, the bulk concentration was increased from zero directly to the desired final concentration, without intermediate steps. A space-time calculation was used to determine when the surfactant solution was introduced into the QCM module and that time was set to zero in all graphs. The residence time of a QCM cell was calculated to be 25 seconds using the QCM module volume of 40 μL above the crystal and the volumetric flow rate. The slopes of adsorption in the different regions were averaged over four crystals in the smooth surface trials and two crystals in the rough surface trials.

At the end of an experiment, a 2% sodium dodecyl sulfate solution was drawn through the tubing and modules for 1 hour followed by pure water for 3 hours, to remove adsorbed CTAB from the tubing and crystal surfaces. Subsequent experiments showed stable baselines

with pure water, indicating adequate removal of any residual surfactant from the equipment.(Shi, et al., 2009)

3. Results and Discussion

3.1 CMC Determination

CMC data, shown in Table 1, report the value and fitting error collected from the specific conductivity method and agree well with values found in literature.(Mata, Varade and Bahadur, 2005; Mukerjee and Mysels, 1971) An increase in bulk solution temperature led to a modest increase in the CMC for CTAB in water due to a decrease in the entropic driving force of micellization as the temperature is increased.(Beyer, Leine and Blume, 2006; Mehta, et al., 2005; Myers, 2006; Ruiz and Molina-Bolivar, 2010)

3.2 Equilibrium Adsorption on Smooth Surfaces

The amount of CTAB adsorbed per unit of nominal smooth surface area vs. bulk concentration is shown in Figure 2a. Concentrations have been normalized to the CMC at each temperature. Below the CMC, as the bulk concentration increased the amount of surfactant adsorbed per area increased for all temperatures, with no statistical difference between the results obtained at different temperatures. Once the CMC was reached all results shown in Figure 2a at temperatures 30 °C and above show a slight maximum in adsorption, followed by a decrease to a plateau as the concentration was increased further. The highest amount adsorbed at the plateau was obtained at 30 °C ($3.1x10^2$ ng/cm^2). As the temperature increased, adsorption decreased, with the minimum obtained at 60 °C (~ $2.1x10^2$ ng/cm^2).

The maximum in adsorption at the CMC is associated with the formation of bulk micelles at the CMC. Maxima in adsorbed mass have also been noted by others, although explanations for the phenomena are varied. (Fava and Eyring, 1956; Furst, et al., 1996; Meader and Fries, 1952;

Paria and Khilar, 2004; Paria, et al., 2005; Sexsmith and White Jr, 1959; Velegol, et al., 2000; Vold and Sivaramakrishnan, 1958) In our case, we believe that surface-active impurities were adsorbing within the supported film below the CMC. Once the CMC is reached, these impurities desorb from the film and partition to the newly formed micelles, yielding a decrease in the mass adsorbed.(Furst, Pagac and Tilton, 1996) Impurities could be isomeric variations of the primary surfactant, which have been suggested to yield the maximum seen for mass adsorbed below the CMC.(Furst, Pagac and Tilton, 1996; Paria, Manohar and Khilar, 2005) A study by Furst et al. also supports the possibility that the maxima were caused by non-surfactant associated impurities. These authors found that maxima in amount adsorbed occurred most often when their silicon surface was exposed to concentrations below the CMC before being increased above the CMC, leaving trace amounts adsorbed following a rinsing step. For surfaces exposed to concentrations above the CMC only, nothing was left on the surface after rinsing, which suggested that any impurities were completely solubilized by micelles in solution.(Furst, Pagac and Tilton, 1996) The impurity in question was later determined as being caused by the poly(vinyl chloride) tubing used in the experimental set-up.(Velegol, et al., 2000)

Our group reported maxima in adsorbed amount near the surfactant CMC previously.(Shi, et al., 2009) Maxima reported in our previous work were much more substantial than those shown here, although the same surfactant and similar surfaces were used.(Wu, et al., 2011) However, previously sonication and helium sparging of the surfactant solutions were not used. We conclude that the sonication/sparging removed impurities from the solutions. Even though we recrystallized three times, a comparison of the amount of surfactant adsorbed to the amount present in solution for adsorption experiments on our relatively flat surfaces suggests that the ratio of impurities to surfactant must be on the order of 1×10^{-5} or less to fully exclude the possibility of impurity adsorption; obtaining this level of purity based on recrystallization

alone is very difficult. This work shows, for the first time to our knowledge, that the majority of surface-active impurities in CTAB after recrystallization are volatile.

Dissipation data as obtained on the smooth surface are shown in Figure 2c. The dissipation, and consequently the morphology, of the adsorbed aggregates were not strongly affected by temperature within the tested temperature range. The greatest dissipation measured was roughly 0.44 $x10^{-6}$ at 30 °C at 2.0 CMC, which is below the criteria reported in the literature for a rigidly bound film (<1.0 $x10^{-6}$).(Mivehi, Bordes and Holmberg, 2011) This low value for the dissipation supports the use of the Sauerbrey equation to determine mass adsorbed from frequency data. As the concentration increased, the dissipation increased for all isotherms. A slight decrease in slope for the dissipation vs. concentration curve was observed once the bulk concentration reached the CMC, but unlike mass adsorbed there was no maximum, suggesting that desorbing impurities had a negligible influence on the flexibility of the supported films. The very slight dissipation increase above the CMC with increasing surfactant concentration is attributed to an increase in the viscosity of the bulk fluid.

3.3 Equilibrium Adsorption on Rough Surfaces

Adsorption isotherms obtained on rough surfaces followed the same trend observed on smooth surfaces. As the bulk concentration increased, mass adsorbed per unit area on the rough surface increased as shown in Figure 2b. In this Figure the nominal surface area is used for estimating the amount adsorbed from the QCM data instead of the actual surface area; the latter requires an assumption such as a fractal surface. (Wu, et al., 2011) When comparing the isotherms above the CMC in Figures 2a and 2b, on average the equilibrium values were lower on the rough surface than the smooth surface, a result our group reported previously.(Shi, et al., 2009; Wu, et al., 2011) This decrease in adsorption is caused by disruption of intermolecular tail-tail interactions by surface roughness.(Fragneto, et al., 1996) Since nominal surface areas were

used in the calculation of the surface area, actual decreases in adsorption densities were larger than shown in the graphs.

On the rough surface, below the CMC mass adsorbed at 30 °C was less than for 40°C and 50 °C. However, mass adsorbed at 30 °C becomes greater than at 40 °C and 50 °C near the CMC. The only peak in mass adsorbed occurs in the 50 °C isotherm, while the other isotherms display rather monotonic transitions to their plateau values. The largest amount of mass adsorbed in the plateau region on the rough surface is $2.8x10^2$ ng/cm^2 and occurs at 30 °C at 1.4 CMC, while the smallest value is $1.6x10^2$ ng/cm^2, found at 60 °C for 1.6 CMC. As with the smooth surface, an increase in temperature led to a decrease in mass adsorbed above the CMC. Data collected on the rough surface shows a greater separation between the 50 °C and 60 °C isotherms, which may be an effect of extra washing cycles increasing the surface roughness, as three extra washing cycles were necessary to repeat the 60 °C trial following the failure of the first trial from bubble formation in the tubing.

Dissipation data collected using the rough surface can be found in Figure 2d. Data are again consistent with a rigidly bound surfactant film on the surface of the crystal. The data did not show any statistical difference between temperatures, except for 50 °C, which showed greater dissipation near the CMC. No observable maximum in dissipation was found. Above the CMC, there was a slight increase in dissipation with increasing concentration, attributable to a slight increase in bulk viscosity. Although we expected that the dissipation would show some evidence of a change induced by an increase in the surface roughness, no statistical distinction between dissipation values gathered on the two surfaces was observed suggesting that the films formed on rough substrates were of similar morphology to those formed on the smooth substrates.

3.4 Time Dependence of Adsorption

3.4.1 Adsorption at 0.1 CMC:

Figure 3 shows the adsorption per nominal surface area from a 0.1 CMC solution at different temperatures on both smooth and rough surfaces as a function of time. Mass adsorbed increased quickly until a plateau was reached for both the smooth and rough surfaces. The plateau in adsorption on the smooth surface decreased with increasing temperature. Surprisingly, on the rough surface the effect of temperature on adsorption was not consistent. The 60 °C isotherm yields the lowest adsorption equilibrium value; the 40 °C and 50 °C curves nearly overlapped and showed greater adsorption than results collected at 30 °C. Based on smooth crystal data the 40 °C and 50 °C equilibrium values should be lower than the 30 °C value. A likely cause is that slight variations in the activity of available surface sites, caused by the cleaning procedure, became more apparent at low surfactant concentrations.

When kinetics results are viewed on a large time scale, Figures 3a and 3b, there appear to be only two regions of adsorption, a region of fast adsorption (~0-200 seconds) and a region of slow adsorption (time>200 sec), which were characterized previously through the use of kinetic models.(Biswas and Chattoraj, 1998; Wu, et al., 2011) When the fast region is viewed on a smaller time scale (Figures 3c and 3d) it becomes apparent that there were actually three regions. These regions have been quantified as 0-10 ng/cm^2 for the first region, 10-50 ng/cm^2 for the second region and above 50 ng/cm^2 for the third region. The first region represents the time interval where the concentration in the cell is changing with time; the residence time of the fluid in the cell is consistent with the time interval characteristic of this first region. At low concentrations, single molecule adsorption can be assumed in this first region. The second region also represents primarily single molecule adsorption. Some cooperative effects could be present, although at 0.1 CMC the number of adsorbed molecules where cooperative effects are significant

is probably small. The third region is dominated by a plateau, indicating that the equilibrium adsorption is being reached.

To examine the differences between adsorption rates in the first two regions a one-step adsorption model, $q_i = q_{i-1} + m_i t_i$, was used.(Biswas and Chattoraj, 1998) In the equation, q_i, m_i and t_i are the mass adsorbed, slope of mass adsorbed over time and time elapsed values for the i^{th} region, while q_{i-1} is the final mass adsorbed value of the preceding region.

Figure 4 reports the average slopes of adsorption for the first region for an increase from pure water to 0.1 CMC on smooth and rough surfaces. This region includes effects related to the flowrate used, but since the flowrate was constant for all trials any measured differences should only reflect differences due to temperature or surface differences. The averages presented are taken over 2 trials (4 crystals per trial) for the smooth crystals and 1 trial (2 crystals per trial) for the rough crystals. As shown in the top portion of Figure 4, no change in slope of mass adsorbed over time was found in this region by varying temperature between 30 °C and 60 °C or by changing the surface roughness.

A higher temperature should lead to faster adsorption in the low concentration region, since the surface is not completely covered and the diffusion constant increases with temperature. Adsorption occurs through single molecule adsorption via electrostatic interactions between the polar head group and charges present on the surface, which are negative from the adsorption of bromide ions. (Mivehi, Bordes and Holmberg, 2011; Paria and Khilar, 2004; Scamehorn, et al., 1982; Somasundaran and Fuerstenau, 1966) However, any expected increase in the kinetics of adsorption is lower than the uncertainty in the measurements as represented by the error bars in Figure 4.

Slopes of adsorption (amount vs. time) in the second region are shown in Figure 5. On the smooth surface the slope was greatest at 30 °C and decreased with increasing temperature.

For the rough surface, the slope at 30 °C was the largest and there was statistically no difference between 40, 50, or 60 °C. On an absolute mass adsorbed basis, the slope on the smooth crystals was higher than that for the rough crystals; this trend was reversed in some cases when taken on a basis of percentage of equilibrium value.

The decrease in slope with increased roughness follows the same trend as was found above the CMC. As adsorption the second region for 0.1 CMC is primarily an enthalpically-driven (i.e. non-cooperative) process, these results indicate that the effects of roughness extend even to regions of adsorption not entropically controlled. A similar finding was expressed previously where adsorption was slowed on a rougher surface by surface rearrangement, even at concentrations well below the CMC.(Wu, et al., 2011) The fact that the kinetics of adsorption decreases with an increase in temperature suggests that the heat of adsorption becomes less exothermic at higher temperature, (Somasundaran and Huang, 2000) which counteracts increases in rate due to a diffusion constant increase. However, in one study with cetylpyridinium chloride, increasing temperature has been shown to lead to more exothermic processes, even though the amounts adsorbed were decreasing.(Seidel, Wittrock and Kohler, 1996)

3.4.2 Adsorption at 1.8 CMC and Two Different Temperatures

To better explore characteristics of other regions at higher concentrations, data for a step increase from pure water to 1.8 CMC were collected at 30 °C and 60 °C on a smooth surface and the associated slopes of adsorption for the different regions are shown in Figure 6. Five regions of adsorption are identified, with the first region beginning at time zero and ending where mass adsorbed is ~10 ng/cm^2. The second and third regions are designated as 10-50 ng/cm^2 and 50-75 ng/cm^2, respectively. The fourth region spans from 75 ng/cm^2 to where mass adsorbed begins to transition to a plateau. The fifth region is where the adsorption slowly approaches a plateau

value. Here the monomer concentration is in such excess that the first region is thought to have an effective concentration of 1.0 CMC almost immediately. The slope of adsorption in this first region appeared to increase with an increase in temperature, whereas at low concentrations there was no observable trend with changing temperature. This behavior is likely an effect of micelles in solution at high concentrations, even though the first region is still single molecule adsorption.(Paria and Khilar, 2004; Scamehorn, Schechter and Wade, 1982; Somasundaran and Fuerstenau, 1966) The slope of the second region was three times higher than that of the first region, where the 60 °C slope is greater than the 30 °C slope. These results support a diffusion controlled adsorption mechanism in the second region, where the increase in temperature caused an increase in the coefficient of diffusion. (Ning, et al., 2006)

The third region observed at the higher concentration is a transition region between the different adsorption mechanisms characteristic of the second and fourth regions. The 30 °C slope in the fourth region increased slightly compared to the second region but was much higher than the 60 °C slope. The decrease in slope of adsorption with temperature indicates that the decrease in driving force for adsorption with an increase in temperature occurs in the same manner as the decrease in the entropic driving force observed for micelle formation in solution. Adsorption is entropically driven at high concentrations, where adsorption in the fourth region is driven by cooperative lateral interactions between surfactants adsorbed on the surface (analogous to Region II of the four-region explanation for isotherms as a function of concentration).(Paria and Khilar, 2004; Somasundaran and Huang, 2000) The lateral interactions are a result of the entropic driving force which occurs as a result of the increase in the entropy gained by water molecules surrounding surfactant tail groups.(Danov and Kralchevsky, 2012; Somasundaran and Huang, 2000) Upon adsorption and organization into a structure where the hydrocarbon chains associate with one another, these water molecules are released from their cage-like structure

surrounding the surfactant, which increases the system entropy because the entropy loss due to the association between the hydrocarbon tails is insignificant compared to the entropy gain of the water.(Fong, 2007) At higher temperatures the entropy gain is lower because the cage-like structure formed by water molecules around a surfactant tail is already less organized at higher temperature. *Figure 6 shows that the overall decrease in adsorption of ionic surfactants with increasing temperature at high surfactant concentration occurs primarily because adsorption is less in the fourth region, where cooperative interactions dominate, due to a decrease in the entropic driving force for adsorption with an increase in temperature.*

The gradual approach to a plateau seen in the fifth region (analogous to region III of the four-region explanation for isotherms as a function of concentration)(Paria and Khilar, 2004) is characteristic of rearrangement of adsorbed surfactant aggregates and filling of remaining surface sites.(Paria and Khilar, 2004; Somasundaran and Fuerstenau, 1966)

The regions described here show similarity to the four-region isotherm developed by Somasundaran and Fuerstenau, with the main difference being the currently presented analysis has a kinetic basis instead of concentration.(Atkin, et al., 2003; Somasundaran and Fuerstenau, 1966) The most notable effect of this difference is the absence of a diffusion controlled region in the four region model which is self-evident since the four-region model is an equilibrium model. The second region results for 0.1 CMC in this work do show agreement with the conclusions of Somasundaran et al. and their respective Region II regarding adsorbed single molecules nucleating increased adsorption.

4. Conclusions

Surfactant adsorption increased with an increase in bulk concentration below the critical micelle concentration (CMC) on both smooth and rough surfaces. At the CMC, on the smooth

surface peaks in mass absorbed were found for all temperatures investigated, while on the rough surface a peak was found only at 50 °C. The cause of peaks in mass adsorbed is the adsorption of surface-active impurities below the CMC, which we previously found to be much more significant on rough surfaces.(Wu, et al., 2011) However, here the peaks were almost eliminated due to helium sparging and bath sonication removing the apparently volatile impurities. To our knowledge, this work represents the first-time surfactant adsorption was studied using QCM at different temperatures, and we found that for this surfactant an increase in temperature caused a reduction in the final equilibrium adsorbed amount on both smooth and rough surfaces, caused by a decrease in the entropic (hydrophobic) driving force of adsorption. As has been found previously, a reduction in amount adsorbed was observed due to roughness. (Fragneto, et al., 1996; Wu, et al., 2011)

Time dependent experiments revealed that at short times after a surface is exposed to surfactant concentrations far below the CMC there were 3 regions of adsorption. In the first region adsorption was diffusion controlled and occurred as the concentration is transitioning from zero (pure water) to 0.1 CMC within the measurement cell. Adsorption in the second region was enthalpically controlled, as the mechanism is single surfactant molecule adsorption via electrostatic interactions. The third region showed slow adsorption to a plateau representing the maximum adsorbed amount under the conditions far below surface saturation. The effect of increasing temperature and roughness was indistinguishable in the first and second regions of adsorption, while both reduced adsorption in the third region. To our knowledge, this kinetic behavior for temperature has never been published previously, while the roughness result is consistent with the room temperature result published previously by our group.(Wu, et al., 2011)

At higher concentrations there were five observable regions, supporting three adsorption mechanisms. In the first and second regions adsorption occurred via a diffusion-controlled

mechanism. The third region was the transition to an entropically controlled, cooperative fourth region, which was then followed by the fifth region, where surface rearrangement occurred. This interpretation is analogous to results presented based on increases in CTAB concentration. (Atkin, et al., 2003; Paria and Khilar, 2004) However, the interesting contribution made by this work is using the time based regional analysis of a single concentration increment at multiple temperatures. This analysis technique led to the unique conclusion that the decrease in mass adsorbed above the CMC with an increase in temperature was attributable to less adsorption in the cooperative fourth region.

References

Alkan, M.; Karadaş, M.; Doğan, M.; Demirbaş, Ö. (2005) Adsorption of CTAB onto perlite samples from aqueous solutions. Journal of Colloid and Interface Science, **291**:309-318. DOI:http://dx.doi.org/10.1016/j.jcis.2005.05.027.

Atkin, R.; Craig, V. S. J.; Wanless, E. J.; Biggs, S. (2003) Mechanism of cationic surfactant adsorption at the solid–aqueous interface. Advances in Colloid and Interface Science, **103**:219-304. DOI:http://dx.doi.org/10.1016/S0001-8686(03)00002-2.

Beyer, K.; Leine, D.; Blume, A. (2006) The demicellization of alkyltrimethylammonium bromides in 0.1M sodium chloride solution studied by isothermal titration calorimetry. Colloids and Surfaces B: Biointerfaces, **49**:31-39. DOI:http://dx.doi.org/10.1016/j.colsurfb.2006.02.003.

Biswas, S. C.; Chattoraj, D. K. (1998) Kinetics of Adsorption of Cationic Surfactants at Silica-Water Interface. Journal of Colloid and Interface Science, **205**:12-20. DOI:http://dx.doi.org/10.1006/jcis.1998.5574.

Bordes, R.; Hook, F. (2010) Separation of Bulk Effects and Bound Mass during Adsorption of Surfactants Probed by Quartz Crystal Microbalance with Dissipation: Insight into Data Interpretation. Analytical Chemistry, **82**:9116-9121. DOI:10.1021/ac1018149.

Bordes, R.; Tropsch, J.; Holmberg, K. (2010) Adsorption of Dianionic Surfactants Based on Amino Acids at Different Surfaces Studied by QCM-D and SPR. Langmuir, **26**:10935-10942. DOI:10.1021/la100909x.

Cademartiri, L.; Ozin, G. A. In *Concepts of Nanochemistry*; Wiley-VCH GmbH & Co., 2009.

Caruso, F.; Serizawa, T.; Furlong, D. N.; Okahata, Y. (1995) Quartz-Crystal Microbalance and Surface-Plasmon Resonance Study of Surfactant Adsorption onto Gold and Chromium-Oxide Surfaces. Langmuir, **11**:1546-1552. DOI:Doi 10.1021/La00005a023.

Danov, K.; Kralchevsky, P. (2012) The standard free energy of surfactant adsorption at air/water and oil/water interfaces: Theoretical vs. empirical approaches. Colloid Journal, **74**:172-185. DOI:10.1134/S1061933X12020032.

Dixit, S. G.; Vanjara, A. K.; Nagarkar, J.; Nikoorazm, M.; Desai, T. (2002) Co-adsorption of quaternary ammonium compounds—nonionic surfactants on solid–liquid interface. Colloids and Surfaces A: Physicochemical and Engineering Aspects, **205**:39-46. DOI:http://dx.doi.org/10.1016/S0927-7757(01)01143-8.

Dominguez, A.; Fernandez, A.; Gonzalez, N.; Iglesias, E.; Montenegro, L. (1997) Determination of Critical Micelle Concentration of Some Surfactants by Three Techniques. Journal of Chemical Education, **74**:1227. DOI:10.1021/ed074p1227.

Fava, A.; Eyring, H. (1956) Equilibrium and Kinetics of Detergent Adsorption-A Generalized Equilibration Theory. Journal of Physical Chemistry, **60**:890-898. DOI:10.1021/j150541a013.

Fong, P. A. (2007). Colloid and Surface Research Trends (Nova Science Publishers.

Fragneto, G.; Thomas, R. K.; Rennie, A. R.; Penfold, J. (1996) Neutron reflection from hexadecyltrimethylammonium bromide adsorbed on smooth and rough silicon surfaces. Langmuir, **12**:6036-6043. DOI:10.1021/la9604644.

Furst, E. M.; Pagac, E. S.; Tilton, R. D. (1996) Coadsorption of Polylysine and the Cationic Surfactant Cetyltrimethylammonium Bromide on Silica. Industrial & Engineering Chemistry Research, **35**:1566-1574. DOI:10.1021/ie9506577.

Gürses, A.; Karaca, S.; Aksakal, F.; Açikyildiz, M. (2010) Monomer and micellar adsorptions of CTAB onto the clay/water interface. Desalination, **264**:165-172. DOI:http://dx.doi.org/10.1016/j.desal.2010.07.022.

Gutig, C.; Grady, B. P.; Striolo, A. (2008) Experimental studies on the adsorption of two surfactants on solid-aqueous interfaces: Adsorption isotherms and kinetics. Langmuir, **24**:13814-13814. DOI:10.1021/la8032034.

Howard, S. C.; Craig, V. S. J. (2009) Very slow surfactant adsorption at the solid-liquid interface is due to long lived surface aggregates. Soft Matter, **5**:3061-3069. DOI:10.1039/b903768c.

Jaschke, M.; Butt, H. J.; Gaub, H. E.; Manne, S. (1997) Surfactant Aggregates at a Metal Surface. Langmuir, **13**:1381-1384. DOI:10.1021/la9607767.

Knag, M.; Sjöblom, J.; Gulbrandsen, E. (2005) The Effect of Straight Chain Alcohols and Ethylene Glycol on the Adsorption of CTAB on Gold. Journal of Dispersion Science and Technology, **26**:207-215. DOI:10.1081/dis-200045595.

Kou, J.; Tao, D.; Xu, G. (2010) A study of adsorption of dodecylamine on quartz surface using quartz crystal microbalance with dissipation. Colloids and Surfaces A: Physicochemical and Engineering Aspects, **368**:75-83. DOI:http://dx.doi.org/10.1016/j.colsurfa.2010.07.017.

Macakova, L.; Blomberg, E.; Claesson, P. M. (2007) Effect of adsorbed layer surface roughness on the QCM-D response: Focus on trapped water. Langmuir, **23**:12436-12444. DOI:10.1021/la7014308.

Manna, K.; Panda, A. (2011) Physicochemical Studies on the Interfacial and Micellization Behavior of CTAB in Aqueous Polyethylene Glycol Media. Journal of Surfactants and Detergents, **14**:563-576. DOI:10.1007/s11743-011-1261-8.

Manojlovic, J. Ž. (2012) The Krafft Temperature of Surfactant Solutions. Thermal Science, **16**:S631-S640. DOI:10.2298/TSCI120427197M.

Marsalek, R.; Pospisil, J.; Taraba, B. (2011) The influence of temperature on the adsorption of CTAB on coals. Colloids and Surfaces A: Physicochemical and Engineering Aspects, **383**:80-85. DOI:http://dx.doi.org/10.1016/j.colsurfa.2011.01.012.

Mata, J.; Varade, D.; Bahadur, P. (2005) Aggregation behavior of quaternary salt based cationic surfactants. Thermochimica Acta, **428**:147-155. DOI:http://dx.doi.org/10.1016/j.tca.2004.11.009.

Meader, A. L.; Fries, B. A. (1952) Adsorption in the Detergent Process. Industrial and Engineering Chemistry, **44**:1636-1648. DOI:10.1021/ie50511a043.

Mehta, S. K.; Bhasin, K. K.; Chauhan, R.; Dham, S. (2005) Effect of temperature on critical micelle concentration and thermodynamic behavior of dodecyldimethylethylammonium bromide and dodecyltrimethylammonium chloride in aqueous media. Colloids and Surfaces A: Physicochemical and Engineering Aspects, **255**:153-157. DOI:http://dx.doi.org/10.1016/j.colsurfa.2004.12.038.

Mivehi, L.; Bordes, R.; Holmberg, K. (2011) Adsorption of Cationic Gemini Surfactants at Solid Surfaces Studied by QCM-D and SPR: Effect of the Rigidity of the Spacer. Langmuir, **27**:7549-7557. DOI:10.1021/la200539a.

Mukerjee, P.; Mysels, K. J. (1971). Critical micelle concentrations of aqueous surfactant systems (U.S. National Bureau of Standards; for sale by the Supt. of Docs., U.S. Govt. Print. Off.

Myers, D. In *Surfactant Science and Technology*; John Wiley & Sons, Inc: Hoboken, New Jersey, 2006.

Ning, H.; Kita, R.; Kriegs, H.; Luettmer-Strathmann, J.; Wiegand, S. (2006) Thermal Diffusion Behavior of Nonionic Surfactants in Water. Journal of Physical Chemistry B, **110**:10746-10756. DOI:10.1021/jp0572986.

Paria, S.; Khilar, K. C. (2004) A review on experimental studies of surfactant adsorption at the hydrophilic solid-water interface. Advances in Colloid and Interface Science, **110**:75-95. DOI:10.1016/j.cis.2004.03.001.

Paria, S.; Manohar, C.; Khilar, K. C. (2005) Adsorption of anionic and non-ionic surfactants on a cellulosic surface. Colloids and Surfaces A: Physicochemical and Engineering Aspects, **252**:221-229. DOI:http://dx.doi.org/10.1016/j.colsurfa.2004.09.022.

Partyka, S.; Lindheimer, M.; Faucompre, B. (1993) Aggregate Formation at the Solid-Liquid Interface-The Calorimetric Evidence. Colloids and Surfaces a-Physicochemical and Engineering Aspects, **76**:267-281. DOI:10.1016/0927-7757(93)80087-u.

Pavan, P. C.; Crepaldi, E. L.; Gomes, G. D.; Valim, J. B. (1999) Adsorption of sodium dodecylsulfate on a hydrotalcite-like compound. Effect of temperature, pH and ionic strength.

Colloids and Surfaces a-Physicochemical and Engineering Aspects, **154**:399-410. DOI:10.1016/s0927-7757(98)00847-4.

Rosen, M. J. In *Surfactants and Interfacial Phenomena*; Wiley and Sons, Inc.: Hoboken, New Jersey, 2004.

Ruiz, C. C.; Molina-Bolivar, J. A. In *Sugar-Based Surfactants: Fundamentals and Applications*; Taylor & Francis: Boca Raton, Fl, 2010.

Sakai, K.; Matsuhashi, K.; Honya, A.; Oguchi, T.; Sakai, H.; Abe, M. (2010) Adsorption Characteristics of Monomeric/Gemini Surfactant Mixtures at the Silica/Aqueous Solution Interface. Langmuir, **26**:17119-17125. DOI:10.1021/la1028367.

Salari, Z.; Ahmadi, M. A.; Kharrat, R.; Shahri, A. A. (2011) Experimental Studies of Cationic Surfactant Adsorption onto Carbonate Rocks. Australian Journal of Applied Sciences, **5**:808-813.

Saphanuchart, W.; Saiwan, C.; O'Haver, J. H. (2007) Effect of adsolubilized solutes on 2-D structure of cationic admicelles. Colloids and Surfaces A: Physicochemical and Engineering Aspects, **307**:71-76. DOI:http://dx.doi.org/10.1016/j.colsurfa.2007.05.018.

Scamehorn, J. F.; Schechter, R. S.; Wade, W. H. (1982) Adsorption of surfactants on mineral oxide surfaces from aqueous solutions: I: Isomerically pure anionic surfactants. Journal of Colloid and Interface Science, **85**:463-478. DOI:http://dx.doi.org/10.1016/0021-9797(82)90013-3.

Seidel, J.; Wittrock, C.; Kohler, H. H. (1996) Adsorption enthalpies of cationic and nonionic surfactants on silica gel. 2. Microcalorimetric determination of adsorption enthalpies. Langmuir, **12**:5557-5562. DOI:10.1021/la960357+.

Sexsmith, F. H.; White Jr, H. J. (1959) The absorption of cationic surfactants by cellulosic materials: III. A theoretical model for the absorption process and a discussion of maxima in absorption isotherms for surfactants. Journal of Colloid Science, **14**:630-639. DOI:http://dx.doi.org/10.1016/0095-8522(59)90028-5.

Shi, L.; Ghezzi, M.; Caminati, G.; Lo Nostro, P.; Grady, B. P.; Striolo, A. (2009) Adsorption Isotherms of Aqueous C12E6 and Cetyltrimethylammonium Bromide Surfactants on Solid Surfaces in the Presence of Low Molecular Weight Coadsorbents. Langmuir, **25**:5536-5544. DOI:10.1021/la8041988.

Smith, T. (1980) The hydrophilic nature of a clean gold surface. Journal of Colloid and Interface Science, **75**:51-55. DOI:http://dx.doi.org/10.1016/0021-9797(80)90348-3.

Somasundaran, P.; Fuerstenau, D. W. (1966) Mechanisms of Alkyl Sulfonate Adsorption at the Alumina-Water Interface. Journal of Physical Chemistry, **70**:90-96. DOI:10.1021/j100873a014.

Somasundaran, P.; Huang, L. (2000) Adsorption/aggregation of surfactants and their mixtures at solid–liquid interfaces. Advances in Colloid and Interface Science, **88**:179-208. DOI:http://dx.doi.org/10.1016/S0001-8686(00)00044-0.

Somasundaran, P.; Krishnakumar, S. (1997) Adsorption of surfactants and polymers at the solid-liquid interface. Colloids and Surfaces a-Physicochemical and Engineering Aspects, **123**:491-513. DOI:10.1016/s0927-7757(96)03829-0.

Stålgren, J. J.; Eriksson, J.; Boschkova, K. (2002) A Comparative Study of Surfactant Adsorption on Model Surfaces Using the Quartz Crystal Microbalance and the Ellipsometer. Journal of Colloid and Interface Science, **253**:190-195.

Suttipong, M.; Grady, B. P.; Striolo, A. (2015) Surfactant Aggregates Templated by Lateral Confinement. Journal of Physical Chemistry B, **119**:5467-5474. DOI:10.1021/jp511427m.

Tummala, N. R.; Grady, B. P.; Striolo, A. (2010) Lateral confinement effects on the structural properties of surfactant aggregates: SDS on graphene. Physical Chemistry Chemical Physics, **12**:13137-13143. DOI:10.1039/C0CP00600A.

Vautier-Giongo, C.; Bales, B. L. (2003) Estimate of the Ionization Degree of Ionic Micelles Based on Krafft Temperature Measurements. Journal of Physical Chemistry B, **107**:5398-5403. DOI:10.1021/jp0270957.

Velegol, S. B.; Fleming, B. D.; Biggs, S.; Wanless, E. J.; Tilton, R. D. (2000) Counterion Effects on Hexadecyltrimethylammonium Surfactant Adsorption and Self-Assembly on Silica. Langmuir, **16**:2548-2556. DOI:10.1021/la9910935.

Vold, R. D.; Sivaramakrishnan, N. H. (1958) The Origin of the Maximum in the Adsorption Isotherms of Association Colloids. Journal of Physical Chemistry, **62**:984-989. DOI:10.1021/j150566a025.

Wall, J. F.; Zukoski, C. F. (1999) Alcohol-Induced Structural Transformations of Surfactant Aggregates. Langmuir, **15**:7432-7437. DOI:10.1021/la980076x.

Wu, S. Q.; Shi, L.; Garfield, L. B.; Tabor, R. F.; Striolo, A.; Grady, B. P. (2011) Influence of Surface Roughness on Cetyltrimethylammonium Bromide Adsorption from Aqueous Solution. Langmuir, **27**:6091-6098. DOI:10.1021/la200751m.

Tables

Table 1 CMC of CTAB measured at various temperatures

Temperature (°C)	CTAB CMC (mM)	Error (mM)
30	0.93	0.03
40	1.02	0.07
50	1.15	0.11
60	1.33	0.13

Figure Legends

Fig. 1 A 2 μm × 2μm AFM image of a smooth gold surface (a), with RMS roughness of 0.9 nm, and a rough gold surface (b) with RMS roughness of 6.07 nm. The images were both obtained with a tip with radius ~8 nm, which must be taken into account when comparing roughness values between measurements.

Fig. 2 Top Row - Surfactant adsorption per unit of nominal surface area vs. bulk concentration normalized by the CMC at, 30, 40, 50, and 60°C on smooth (a) and rough (b) gold surfaces. Bottom Row - Dissipation vs. bulk concentration normalized to CMC at each temperature on smooth (c) and rough (d) surfaces

Fig. 3 Mass CTAB adsorbed per unit of nominal surface area as a function of time on both smooth (a, c) and rough (b, d) surfaces at 0.1 CMC

Fig. 4 Average slopes of adsorption in areal mass per time and percent of equilibrium coverage in the first region for 30, 40, 50, and 60°C isotherms (left to right respectively) for a bulk concentration of 0.1 CMC on the smooth and rough gold surfaces

Fig. 5 Average slopes of adsorption in the second region for 30, 40, 50, and 60°C (left to right respectively) for a bulk concentration of 0.1 CMC on smooth and rough gold surfaces

Fig. 6 (a) Mass of CTAB adsorbed as a function of time on a smooth gold surface at 30 and 60°C. (b) Average slopes of adsorption in the 1st, 2nd and 4th regions (left to right, respectively) at 30°C and 60°C for a bulk concentration of 1.8 CMC on a smooth gold surface

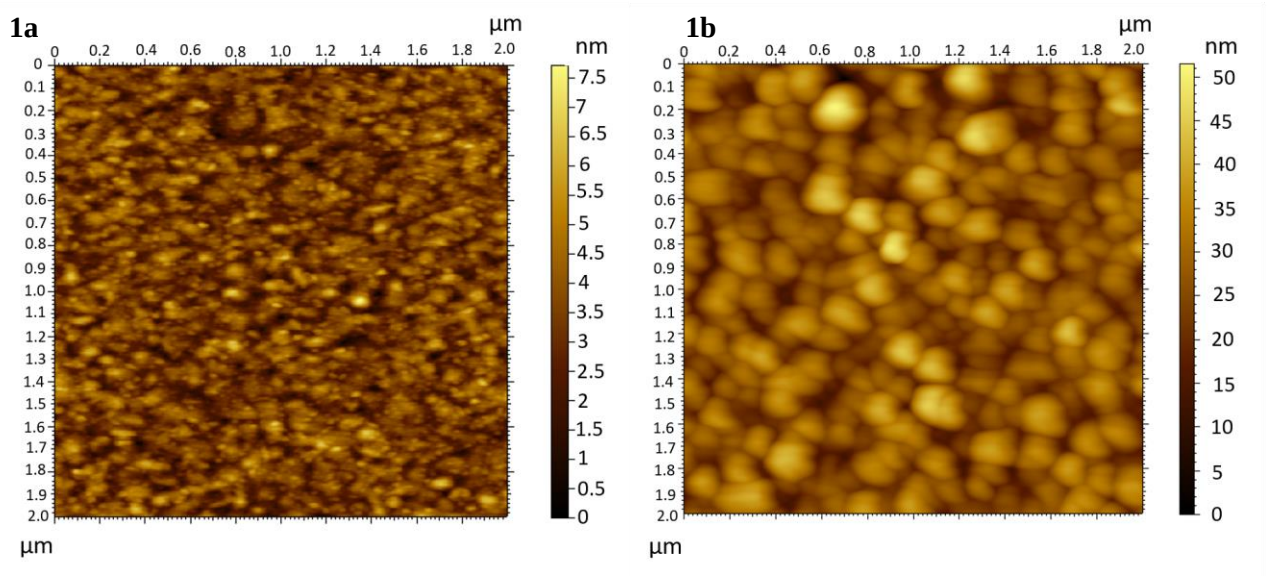

Fig. 1

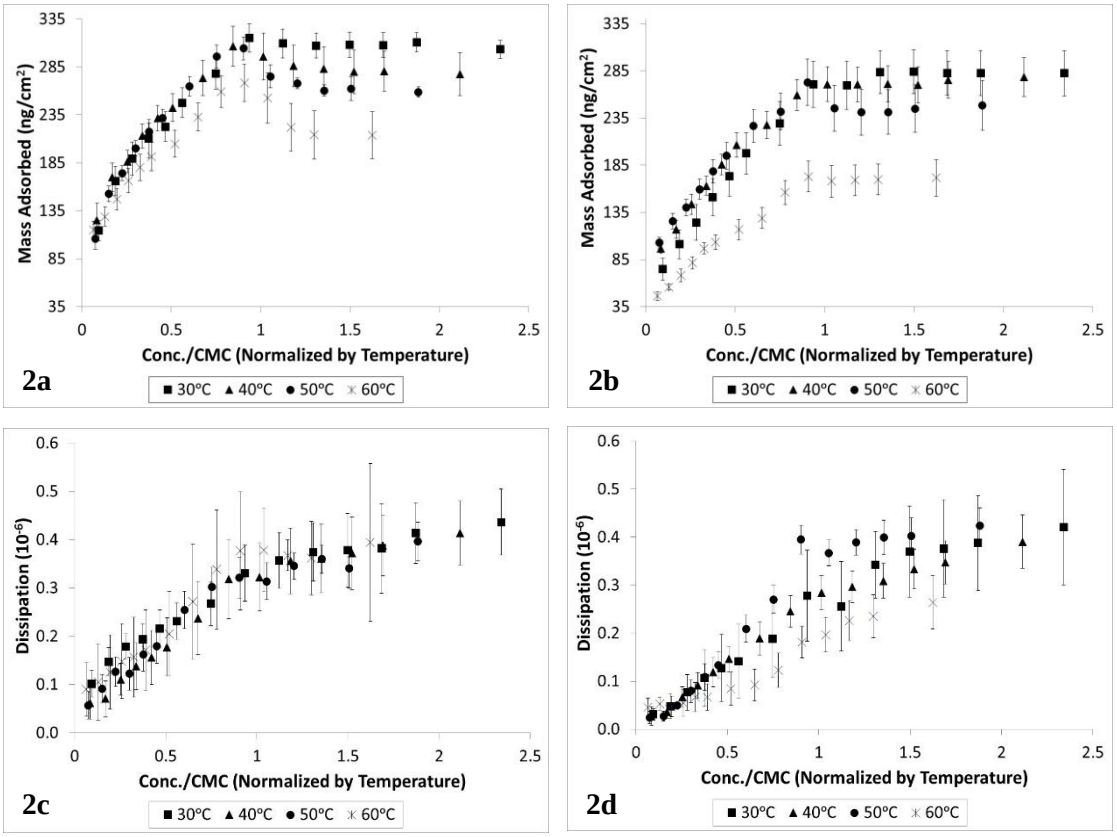
Mass Adsorbed (ng/cm²)
335
285
235
185
135
85
35
0
0.5
1
1.5
2
2.5
Conc./CMC (Normalized by Temperature)
30°C 40°C 50°C 60°C
2a
2b
Dissipation (10⁻⁶)
0.6
0.5
0.4
0.3
0.2
0.1
0.0
2c
2d

Fig. 2

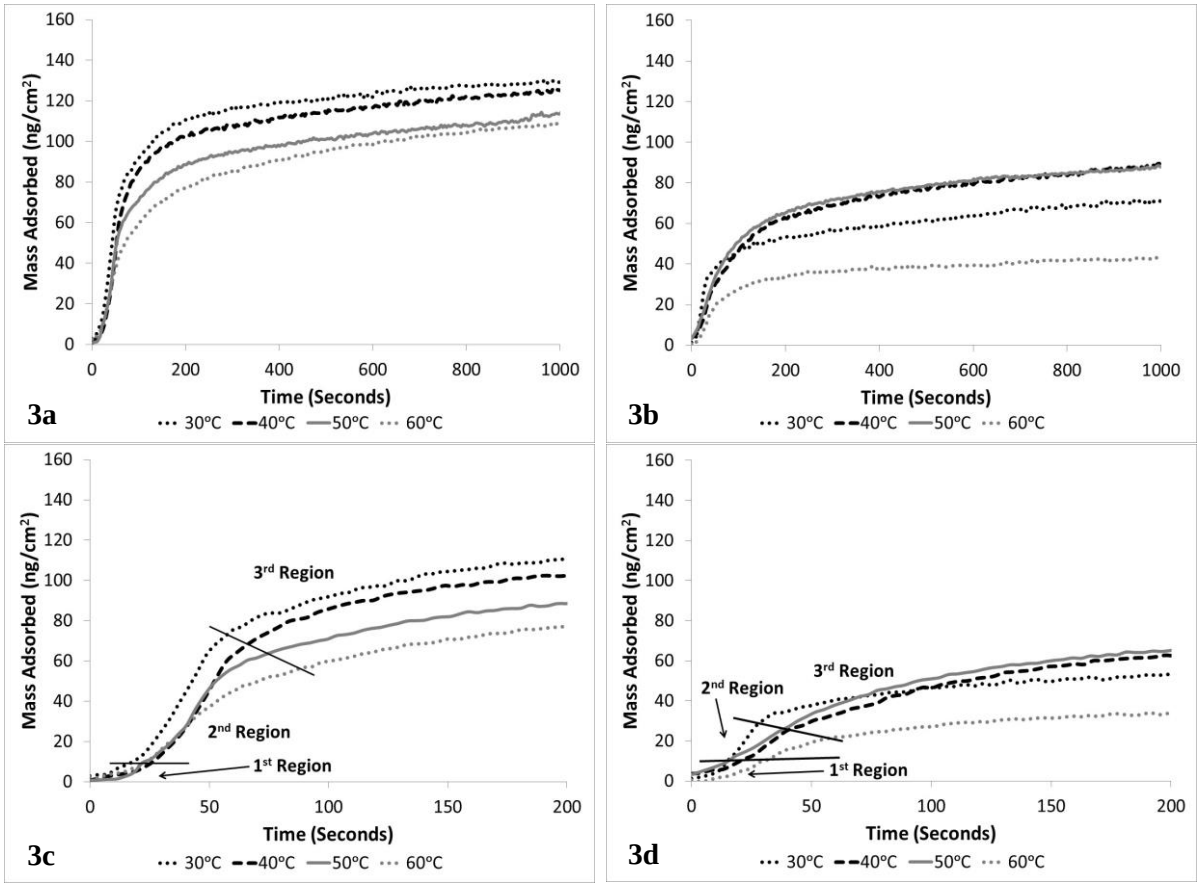
Mass Adsorbed (ng/cm²)
Time (Seconds)
3a
3b
3c
3d
30°C
40°C
50°C
60°C
1st Region
2nd Region
3rd Region

Fig. 3

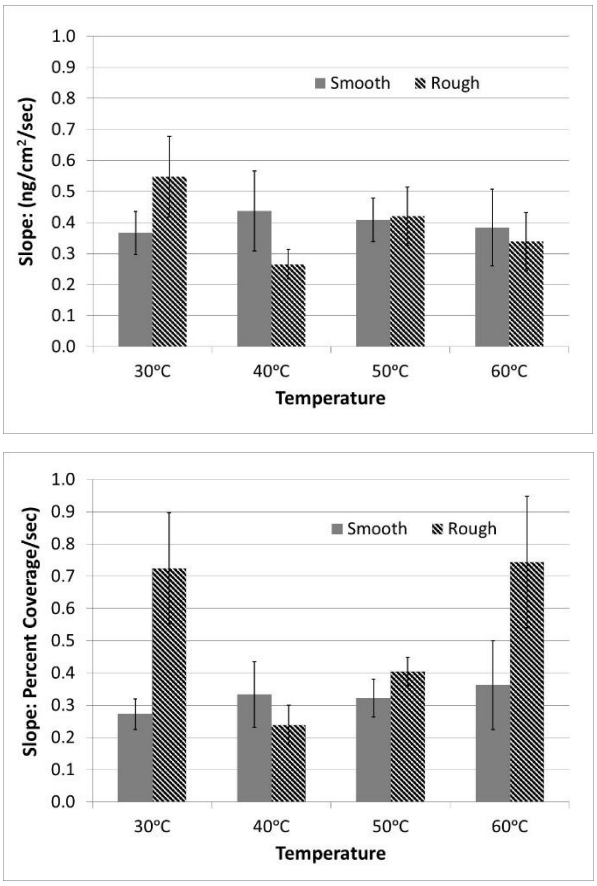
1.0
0.9
0.8
0.7
0.6
0.5
0.4
0.3
0.2
0.1
0.0
Smooth
Rough
Slope: (ng/cm²/sec)
30°C
40°C
50°C
60°C
Temperature
Slope: Percent Coverage/sec)

Fig. 4

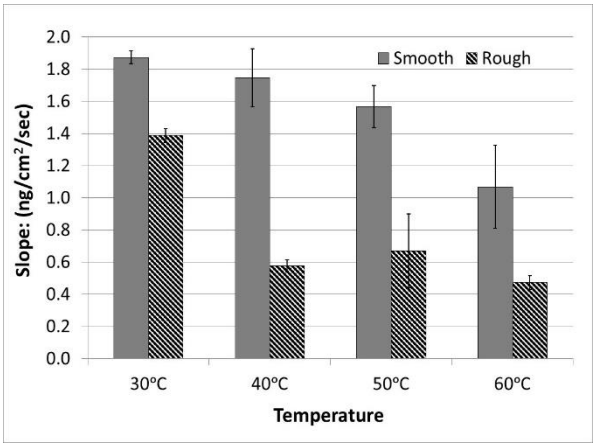
2.0
1.8
1.6
1.4
1.2
1.0
0.8
0.6
0.4
0.2
0.0
Slope: (ng/cm²/sec)
Smooth
Rough
30°C
40°C
50°C
60°C
Temperature

,

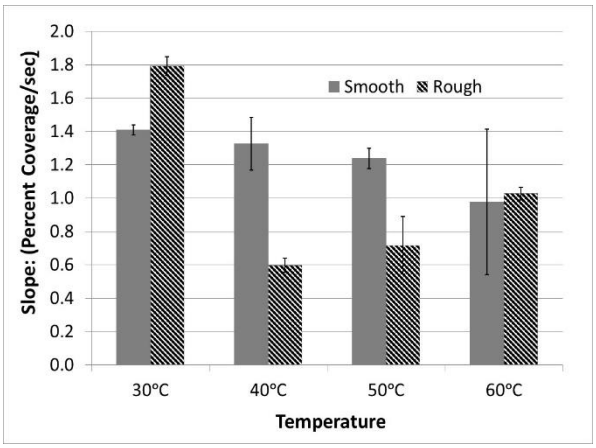
2.0
1.8
1.6
1.4
1.2
1.0
0.8
0.6
0.4
0.2
0.0
Slope: (Percent Coverage/sec)
Smooth
Rough
30°C
40°C
50°C
60°C
Temperature

Fig. 5

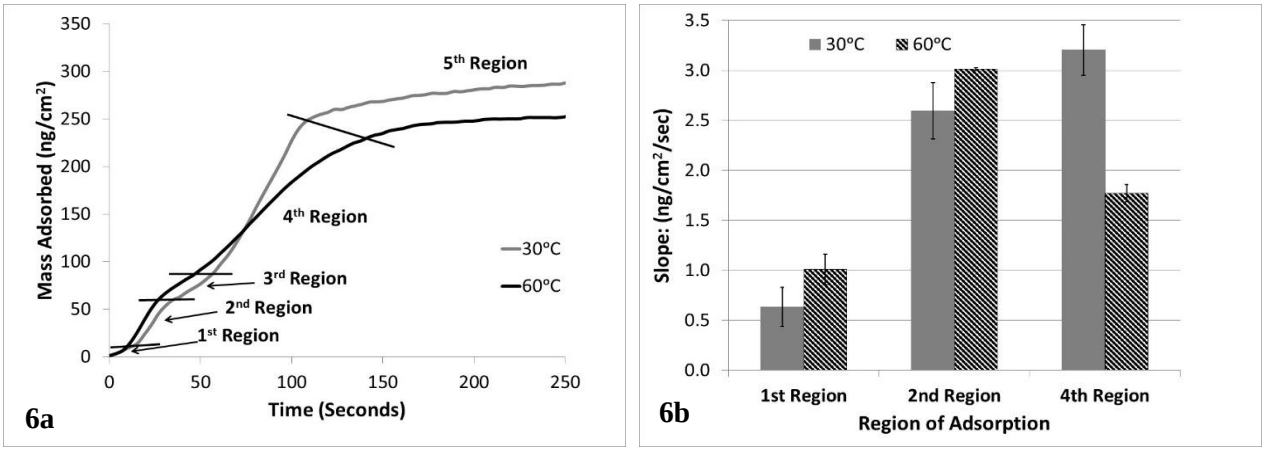
Mass Adsorbed (ng/cm²)
Time (Seconds)
5th Region
4th Region
3rd Region
2nd Region
1st Region
30°C
60°C
6a
Slope: (ng/cm²/sec)
30°C
60°C
1st Region
2nd Region
4th Region
Region of Adsorption
6b

Fig. 6